Spectrochimica Acta, Vol. 29A, pp. 1733 to 1743. Pergamon Press 1973. Printed in Northern Ireland

A vibrational study of ferrocene and ruthenocene

J. S. BODENHEIMER* and W. LOW
Microwave Division, The Racah Institute of Physics, The Hebrew University, Jerusalem, Israel

(*Received* 27 *December* 1972)

Abstract—The vibrational modes of "sandwich" molecules are reviewed. Selection rules for ferrocene and ruthenocene crystals are given, including the lattice modes. Spectra at 80°K are presented, as well as the low frequency spectrum of ferrocene at various temperatures from 180 to 80°K. A comparative assignment of the molecular vibrations for ferrocene and ruthenocene is tabulated. In both cases the ring tilt mode ν_{21} is higher in frequency than the metal-ring stretching modes.

INTRODUCTION

MANY di*cyclo*pentadienyl–metal molecules have been synthesised, but most decompose rapidly under atmospheric conditions. The most stable are ferrocene $[Fe(C_5H_5)_2]$ and ruthenocene $[Ru(C_5H_5)_2]$, both of which can easily be kept at room conditions. Considerable interest in these compounds has been aroused by the unusual structure of the molecules, in which two five-fold aromatic C_5H_5 rings "sandwich" the metal atom. However in ferrocene crystals it appears that the rings conform in an antiprismatic (staggered) structure [1], whereas in ruthenocene crystals the molecule assumes a prismatic (eclipsed) structure [2] (Fig. 1). Furthermore, electron diffraction studies [3] have shown that in the gas phase ferrocene assumes the prismatic form. Various low temperature anomalies in ferrocene have been discovered and investigated [4–6] but no similar phenomena have been found in ruthenocene.

Raman and infrared spectra of ferrocene and ruthenocene have been reported previously by several workers [7–11], and the main features of the controversial original assignment given by NELSON and LIPPINCOTT are now considered to be valid.

Laser Raman spectra of ferrocene and ruthenocene single crystals have been presented and assigned in two preliminary reports [12, 13]. In this paper the results

* Present address: Department of Physics, Wheatstone Laboratory, King's College, Strand, London WC2R 2LS.

[1] J. D. DUNITZ, L. E. ORGEL and A. RICH, *Acta Cryst.* **9**, 373 (1956).
[2] G. L. HARDGROVE and D. H. TEMPLETON, *Acta Cryst.* **12**, 28 (1959).
[3] A. HAALAND and J. E. NILSSON, *Acta Chem. Scand.* **22**, 2653 (1968).
[4] J. W. EDWARDS, G. L. KINGTON and R. MASON, *Trans. Faraday Soc.* **56**, 660 (1960).
[5] L. N. MULAY and A. ATTALLA, *J. Am. Chem. Soc.* **85**, 702 (1963).
[6] J. S. BODENHEIMER and W. LOW, *Phys. Lett.* **36A**, 253 (1971).
[7] E. R. LIPPINCOTT and R. D. NELSON, *Spectrochim. Acta* **10**, 307 (1958).
[8] W. K. WINTER, B. CURNUTTE and S. E. WHITCOMB, *Spectrochim. Acta* **12**, 1085 (1959).
[9] H. P. FRITZ, *Adv. Organometal. Chem.* **1**, 239 (1964).
[10] T. V. LONG and F. R. HUEGE, *Chem. Commun.* **20**, 1239 (1968).
[11] D. HARTLEY and M. J. WARE, *J. Chem. Soc. A* 138 (1969).
[12] J. S. BODENHEIMER, E. LOEWENTHAL and W. LOW, *Chem. Phys. Lett.* **3**, 715 (1969).
[13] J. S. BODENHEIMER, *Chem. Phys. Lett.* **6**, 519 (1970).

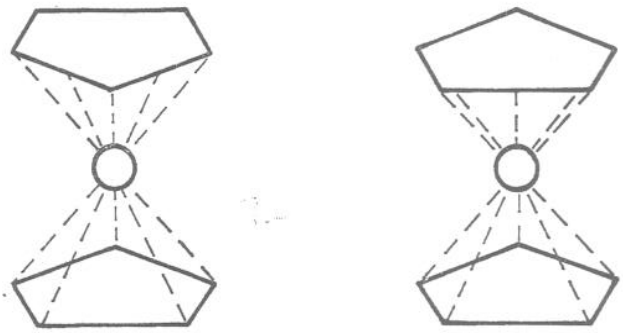

Fig. 1. The two forms of sandwich structure of metallocene molecules: (a) D_{5d}, antiprismatic (b) D_{5h}, prismatic.

of a comparative study are given, which substantiate these previous reports. Since assignment of the molecular modes in ruthenocene has very recently been discussed comprehensively by Adams and Fernando [14], we do not discuss assignments further, except for certain points of interest—in particular the frequencies of the "ring tilt" and "metal-ring stretch" modes.

Molecular Selection Rules

The "sandwich" structure of metallocenes corresponds to the D_{5h} point group for prismatic molecules, and to D_{5d} symmetry for antiprismatic molecules. The selection rules are:

$$D_{5h}: \; 4A_1' + 2A_1'' + A_2' + 4A_2'' + 5E_1'' + 6E_1' + 6E_2' + 6E_2''$$

$$D_{5d}: \; 4A_{1g} + 2A_{1u} + A_{2g} + 4A_{2u} + 5E_{1g} + 6E_{1u} + 6E_{2g} + 6E_{2u}$$

activity: R ia ia i.r. R i.r. R ia

Methods of factor group analysis were extended to verify the correlation between D_{5d} modes and D_{5h} modes. This is based on an imaginary intermediate state D_5 in which one ring is rotated by an arbitrary angle θ with respect to the other. Starting from a D_{5h} molecule, where $\theta = 0$, one ring is rotated by an arbitrary angle $0 < \theta < \pi/5$ so that the symmetry becomes D_5. Using correlation tables [15], correlations can be drawn between the species of the two symmetries. Now the ring is rotated further to $\theta = \pi/5$ where the symmetry becomes D_{5d}, and the correlation can be completed. From the correlation it is found that the D_{5h} species $A_1'A_1''$, $A_2'A_2''$, $E_1''E_1'$, $E_2'E_2''$ correspond to the D_{5d} species $A_{1g}A_{1u}$, $A_{2g}A_{2u}$, $E_{1g}E_{1u}$, $E_{2g}E_{2u}$ respectively.

The vibrations can be divided for descriptional purposes into two types: intra-ring modes which can be described as motions within the C_5H_5 rings, and inter-ring modes which are skeletal movements involving the rings and the metal atom. Such a description of the modes in both symmetries (which assumes no mixing of modes)

[14] D. M. Adams and W. S. Fernando, *J. Chem. Soc. Dalton Trans.* 2507 (1972).
[15] E. B. Wilson, J. C. Decius and P. C. Cross, *Molecular Vibrations*, McGraw-Hill, New York (1955).

is given in Table 1, following FRITZ [9]. The numbering of the modes is in accordance with Ref. [7]. Modes 4, 6, 11, 16, 21, 22 are of an inter-ring character; all the other modes are intra-ring motions. The two mode numbers (on the right and left hand sides of the table) which correspond to each intra-ring mode description refer to the multiplicity caused by the existence of two rings: one mode corresponds to an in-phase movement of the rings, the other to out-of-phase motion. The energy difference between these two forms of motion depends on the interaction between the rings. The interaction between the rings in the molecule is relatively weak, so where one mode is Raman active and the other i.r. active near coincidences should occur in the Raman and i.r. solution spectra. On the other hand, coincidences are not expected for the external ring vibrations, although the frequencies of similar modes may be close to each other. A point group analysis for D_{5h} and D_{5d} is given in Table 2.

CRYSTAL SELECTION RULES

(a) Ferrocene crystallises in the monoclinic space group C_{2h}^5, with two molecules per unit cell. The cell constants are $a = 10{\cdot}561$ Å, $b = 7{\cdot}597$ Å, $c = 5{\cdot}952$ Å, $\beta = 121{\cdot}02°$ [1]. The site group is C_i and the correlation diagram $D_{5d} \rightarrow C_i \rightarrow C_{2h}^5$ is given in Table 3. The Raman and i.r. activities are also given. The degeneracies present in the molecule are removed under the site symmetry. Furthermore, each site vibration corresponds to two crystal vibrations because of the two molecules per unit cell. Parity is conserved throughout the diagram.

All even parity (g) molecular vibrations are Raman active in the crystal, and all odd parity (u) vibrations are i.r. active. Thus in addition to the D_{5d} Raman active modes which are all Raman active in the crystal, the D_{5d} inactive ν_7 becomes Raman active. Likewise, the inactive A_{1u} and E_{2u} modes become i.r. active in the crystal.

(b) Ruthenocene crystallises in the orthorhombic space group D_{2h}^{16}, with four molecules per unit cell. The cell constants are $a = 7{\cdot}13$ Å, $b = 8{\cdot}99$ Å, $c = 12{\cdot}81$ Å [2]. The four ruthenium atoms lie on reflection planes σ_{ac}. These planes coincide with a σ_v reflection plane of the molecule. The site group is therefore C_s, and the correlation diagram $D_{5h} \rightarrow C_s(\sigma_{ac}) \rightarrow D_{2h}^{16}$ is given in Table 4. Every site vibration corresponds to four crystal vibrations because of the four molecules per unit cell, and all the molecular vibrations have both Raman and i.r. active correspondents in the space group. Near coincidences are expected between groups of frequencies corresponding to in-phase and out-of-phase ring modes, as in the molecules. However it seems reasonable to assume, as do ADAMS and FERNANDO [14], that frequencies corresponding to point group Raman active modes are more likely than other modes to appear in the solid state Raman spectrum.

EXPERIMENTAL

Single crystals of ferrocene were grown from solution in benzene, toluene, carbon tetrachloride and ethanol. By far the best crystals were obtained from toluene solution. Previous workers have used mainly benzene and ethanol. Ferrocene crystals grow in parallelepipeds or needles, with facets $(1\bar{1}0)$, (110), (001). The needle axis is [001]. The bisectors of the (001) parallelogram were taken as the [010] and [100] axes. Because of the orange colour of the crystals, the 6328 Å line of a He–Ne laser was used, with 10–20 mW at the crystal.

Table 1. Description of the vibrations in ferrocene and ruthenocene molecules

D_{5h}	D_{5d}	Frequency No.	Description	Frequency No.	D_{5d}	D_{5h}
A_1'	A_{1g}	1	CH stretch	8	A_{2u}	A_2''
		2	CH bend(⊥)	9		
		3	Ring breath	10		
		4	M–ring stretch	11		
A_2'	A_{2g}	7	CH bend(∥)	5	A_{1u}	A_1''
			Torsion	6		
E_1''	E_{1g}	12	CH stretch	17	E_{1u}	E_1'
		13	CH bend (∥)	18		
		14	CH bend (⊥)	19		
		15	CC stretch	20		
		16	Ring tilt	21		
			Ring M–ring bend	22		
E_2'	E_{2g}	23	CH stretch	29	E_{2u}	E_2''
		24	CH bend (∥)	30		
		25	CH bend (⊥)	31		
		26	CC stretch	32		
		27	Ring distortion(∥)	33		
		28	Ring distortion(⊥)	34		

Notation: C_5H_5–Metal–C_5H_5 Inter-ring modes, 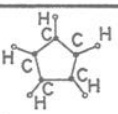 Intra-ring modes

∥ and ⊥ are respective to the ring plane.

Table 2. Point group analysis for ferrocene and ruthenocene molecules. α_{ij} and M_i components refer to Raman and infrared activity. T_i and R_i refer to translations and rotations respectively

Species			Number of	Vibrations			
D_{5d}	D_{5h}	Activity	Modes	Inter-ring	Intra-ring	Rot.	Trans.
A_{1g}	A_1'	$\alpha_{xx} + \alpha_{yy}$, α_{zz}	4	1	3	—	—
A_{1u}	A_1''	—	2	1	1	—	—
A_{2g}	A_2'	R_z	2	—	1	1	—
A_{2u}	A_2''	T_z, M_z	5	1	3	—	1
E_{1g}	E_1''	(R_x, R_y), $(\alpha_{yz}, \alpha_{zx})$	6	1	4	1	—
E_{1u}	E_1'	(T_x, T_y), (M_x, M_y)	7	2	4	—	1
E_{2g}	E_2'	$(\alpha_{xx} - \alpha_{yy}, \alpha_{xy})$	6	—	6	—	—
E_{2u}	E_2''	—	6	—	6	—	—

Table 3. Correlation scheme for ferrocene. The molecular axes are designated xyz (where z is perpendicular to the ring planes) and the crystal axes are abc (where b is the symmetry axis)

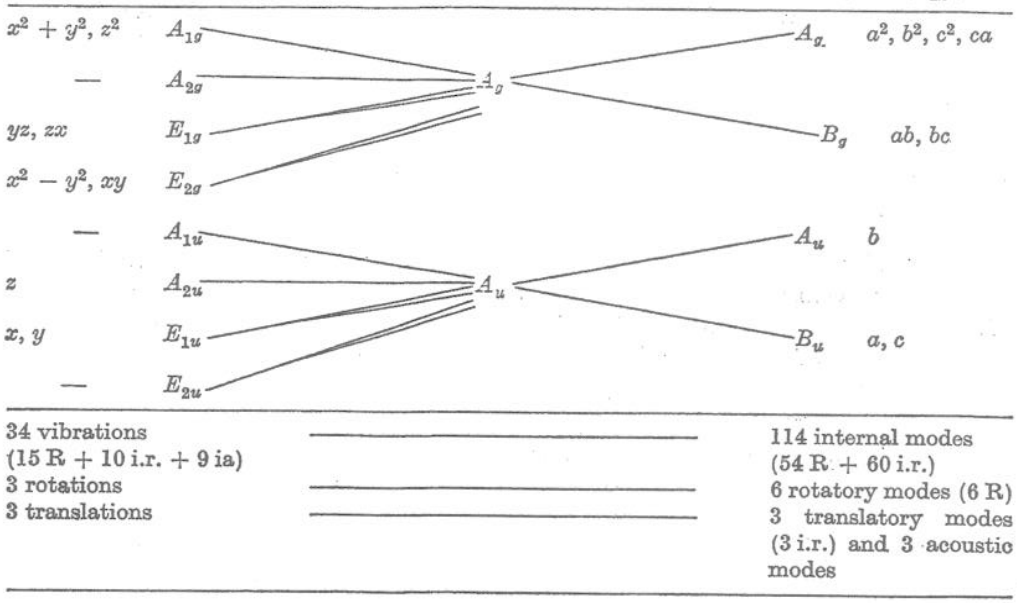

Single crystals of ruthenocene were grown from solution in toluene. The crystals grew in decahedrons with bases parallel to (001). The bisectors of these bases were taken as the axes [010], [100]. 500mW of the 4880 Å line of an argon laser did not appear to damage the crystals.

For all the low temperature measurements a self-contained gas flow cryostat was used. Due to special construction of the cryostat, the specimen is easily accessible externally for alignment or replacement. The basic detection system consisted of a selected Philips XP1117 uncooled photomultipler, d.c. amplification and an X–Y chart recorder. The accuracy in frequency measurements was better than ± 2 cm^{-1}.

Table 4. Correlation scheme for ruthenocene

Molecule (D_{5h})		Site (C_s)	Crystal (D_{2h}^{16})	
x^2+y^2, z^2	A_1'	A'	A_g	a^2, b^2, c^2
—	A_2'		B_{1g}	ab
x, y	E_1'		B_{2g}	ca
x^2-y^2, xy	E_2'		B_{3g}	bc
—	A_1''	A''	A_u	
z	A_2''		B_{1u}	a
yz, zx	E_1''		B_{2u}	b
—	E_2''		B_{3u}	c
34 vibrations (15 R + 10 i.r. + 9 ia)			228 internal modes (114 R + 88 i.r. + 26 ia)	
3 rotations			12 rotatory modes (6 R + 4 i.r. + 2 ia)	
3 translations			9 translatory modes (6 R + 2 i.r. + 1 ia) and 3 acoustic modes	

Polarization characteristics of blazed diffraction gratings present a problem well known to spectroscopists. The efficiency of gratings below the blaze wavelength is higher for radiation with electric field vector parallel to the grating grooves, but above blaze wavelength the efficiency is higher for electric field vector perpendicular to the grooves. This effect is magnified by the use of two gratings in double monochromators. However advantage was taken of 1200 line/mm gratings blazed at 10000 Å. With the 4880 Å exciting line using the second order of the monochromator the spectrum is conveniently close to the blaze wavelength. But for excitation at 6328 Å, the Raman spectrum in the first order of the monochromator falls well below this wavelength, whereas in the second order the spectrum is well above it. For polarization measurements where the **E** vector is parallel to the monochromator slits (and grating grooves), the first order of the monochromator was used. For measurements where **E** is perpendicular to the slits, the second order was used. This resulted in a fivefold improvement in signal. Investigation of the high frequency bands (~3000 cm^{-1}) with the He–Ne laser was slightly impeded by loss of sensitivity in S20 photomultiplier response.

Results

Raman spectra of ferrocene and ruthenocene were obtained at various temperatures from room temperature down to 80°K. Spectra obtained at 80°K are presented in Figs. 2 and 3 and the results are tabulated in Table 5.

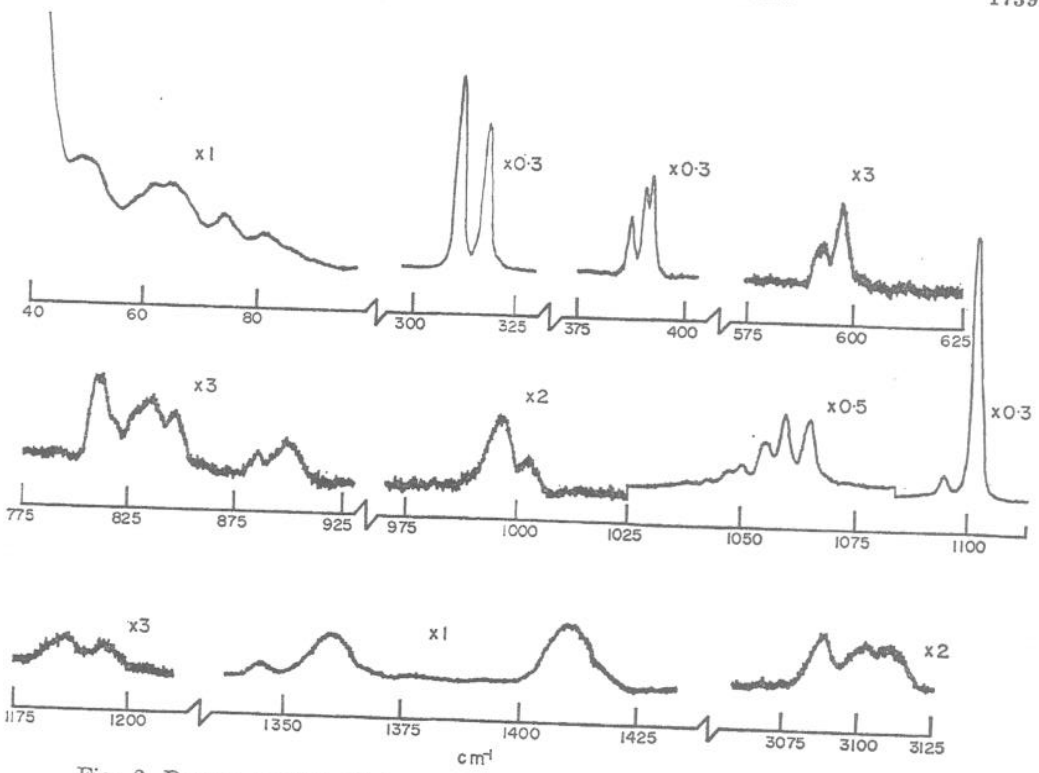

Fig. 2. Raman spectra of ferrocene crystals at 80°K. Multiplication factors refer to relative signal gain.

Table 5. Measured frequencies (cm^{-1}) of ferrocene and ruthenocene single crystals at 80°K

Ferrocene	Ruthenocene	General description
48? 57, 65, 73, 82	49?, 53, 57, 60, 64?, 70, 75, 78, 80, 86	Intermolecular modes
	130	
309, 316 388, 392, 393	329, 336 392, 394?, 403, 404, 400, 407	Ring external modes
593, 598 808, 814 823?, 826?, 834, 843 884, 898 996, 1003 1042, 1046, 1049 1054, 1058, 1063 1095, 1102 1187, 1195	602, 607 818 832, 834, 841, 846 868, 896, 909 991. 996, 998?, 1003, 1012 1049, 1062, 1065, 1068 1092, 1099, 1101 1169?, 1176?, 1184, 1194, 1203, 1208	Intra ring bending and distortion modes
1346, 1360 1410	1359, 1365 1404, 1407, 1411, 1414	Intra ring CC stretching modes
	2736, 2739, 2746	Difference bands (at room temp. only)
3088 3102 3114	3076, 3083, 3085 3092, 3098, 3102 3104, 3112, 3113	Intra ring CH stretching modes

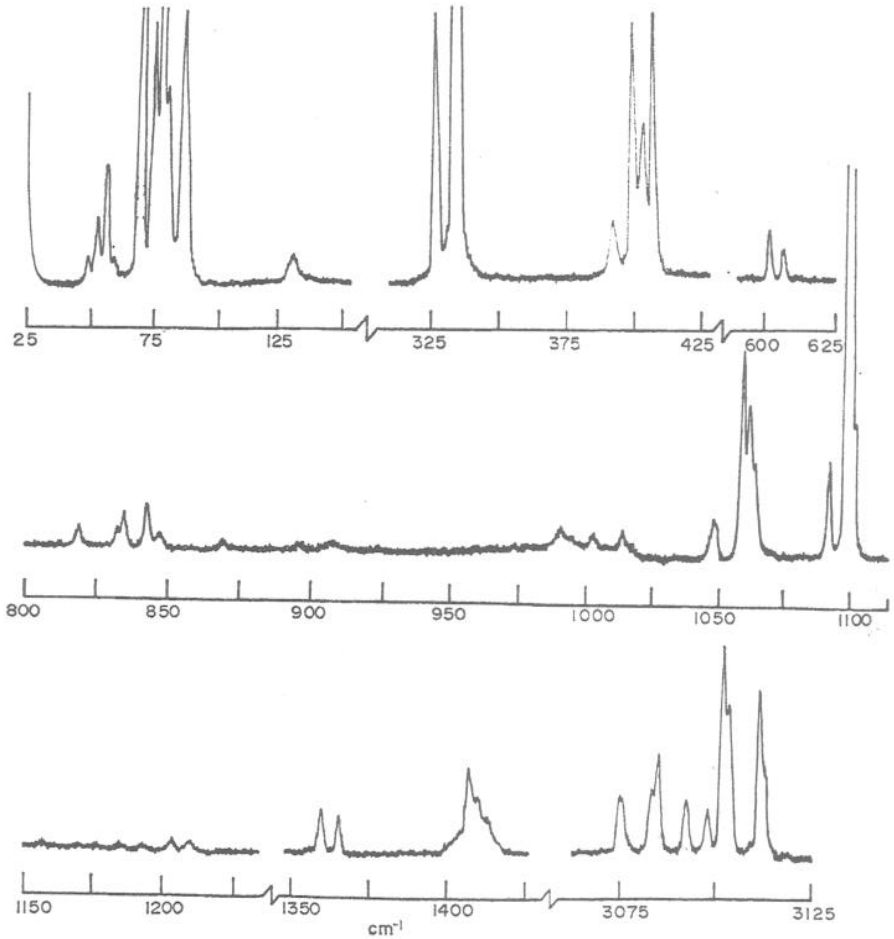

Fig. 3. Raman spectra of ruthenocene crystals at 80°K.

The bands at frequencies above 100 cm^{-1}, which are associated with molecular modes, become sharper with decreasing temperature, whereas the bands below 100 cm^{-1}, which are associated with lattice modes, become less intense with decreasing temperature. Frequency shifts between 300 and 80°K were generally smaller than 5 cm^{-1}.

In contrast to the molecular internal modes, which are similar in the two sets of spectra except for increased splitting in ruthenocene, the lattice modes are markedly different. In ferrocene these modes are weak and broad, whereas in ruthenocene they are intense and sharp. Low frequency spectra of ferrocene at temperatures from 180 to 80°K are shown in Fig. 4. These spectra were obtained consistently from various minute crystal fragments ($\sim$0·1 mm^3). Polarized spectra obtained from well shaped unshattered crystals at 180°K are shown in Fig. 5. At first sight the two figures seem unrelated. However if the ghost curve in Fig. 6 is subtracted from the fragment spectra (since the jagged edges cause strong reflections) the two sets of spectra are comparable. The features at 48, 60 and 97·5 cm^{-1} in Fig. 4 appear to

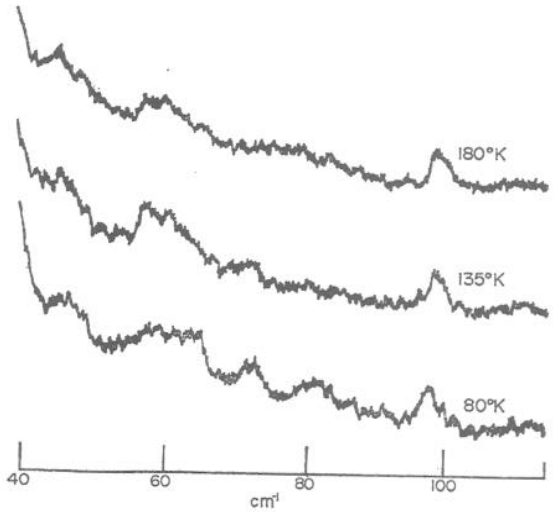

Fig. 4. Low frequency Raman spectra of ferrocene crystal fragments, showing the intermolecular modes at 180, 135 and 80°K. Slits 2 cm^{-1}, integration time 3 sec.

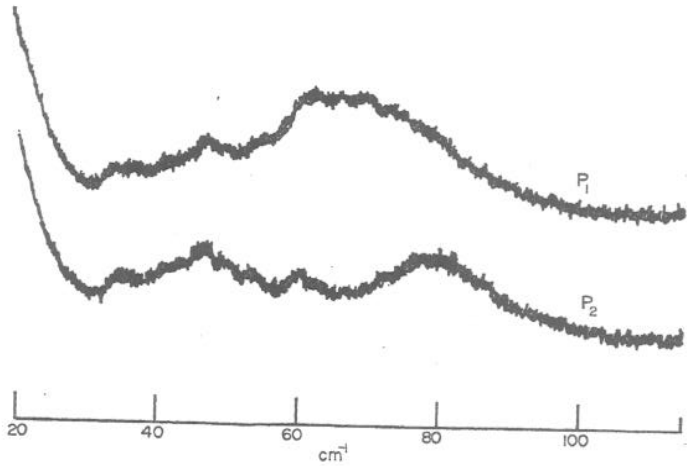

Fig. 5. Low frequency Raman spectra from an unshattered crystal at 180°K, showing the intermolecular modes in two polarizations: p_1 (bb) and $p_2(bc)$. Slits 2·5 cm^{-1}, integration time 3 sec.

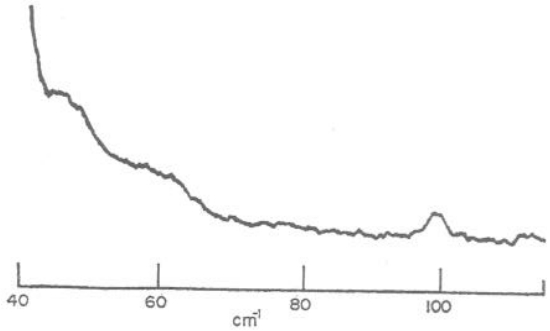

Fig. 6. Ghost curve of the spectrophotometer with He–Ne laser, 2 cm^{-1} slits.

Table 6. Vibrational assignments (cm^{-1}) for ferrocene and ruthenocene molecules in the solid state

ν	Ferrocene	Ruthenocene	ν	Ferrocene	Ruthenocene
1	3110	3112	8	3103	3100
2	814	818	9	820	808
3	1102	1100	10	1110	1095
4	309	333	11	478	380
7	1250	1250	5	1255	1255
			6	—	130
12	3086	3084	17	3077	3076
13	998	1000	18	1005	1005
14	844	842	19	855	834
15	1410	1410	20	1410	1410
16	389	400	21	492	450
			22	179	170
23	3100	3104	29	3085	3092
24	1191	1205	30	1189	1188
25	1058	1065	31	1055	1050
26	1356	1360	32	1351	1360
27	897	900	33	885	868
28	597	603	34	569	600

be spurious. In fact the 97·5 cm^{-1} band corresponds to a neon discharge line. From Fig. 5, which is essentially ghost free, it appears that the 60 cm^{-1} feature is only partly due to a ghost. There is some doubt whether the feature at 48 cm^{-1} is a Raman band or not. The 60 cm^{-1} band is narrower in the fragment, and splits into two unresolved lines at 57 and 65 cm^{-1} at 80°K. Two additional lines at 73 and 82 cm^{-1} become evident below 135°K. These lines replace a broad feature (too weak to be observed in the fragment at 180°K) which occurs in the P_2 polarization of Fig. 5.

A complete assignment of the molecular vibrations for ferrocene and ruthenocene is given in Table 6. The frequencies listed are room temperature values, and for multiplet lines the given frequency represents the peak at low resolution. Thus the frequencies are indicative of the energies of the molecular modes. On comparison of the right and left hand columns of the table it is evident that for intra-ring modes (see Table 1) the in-phase and out-of-phase frequencies are nearly coincident. However it is noteworthy that in ruthenocene, most intra-ring modes which are inactive or i.r. active in the molecular symmetry are of slightly lower frequency than the corresponding Raman modes, e.g. $\nu_1 > \nu_8$, $\nu_{14} > \nu_{19}$, $\nu_{25} > \nu_{31}$, $\nu_{27} > \nu_{33}$. This must be due to the inter-ring exchange energy being positive for the one type of motion and negative for the other, in the prismatic (D_{5h}) configuration. ν_5 is observed in the infrared at 1257 cm^{-1} for ferrocene [8] and at 1251 cm^{-1} for ruthenocene [14]. This invalidates our previous tentative assignment of ν_7 to frequencies near 1095 cm^{-1}, and it is therefore reassigned to 1255 cm^{-1} for both cases.

The inter-ring modes are not expected to be mutually coincident. Inspection of table 1 leads to the prediction $\nu_4 < \nu_{11}$ and $\nu_{16} < \nu_{21}$. In ruthenocene ADAMS and FERNANDO [14] have reassigned the ν_{11} and ν_{21} modes to frequencies 450 and 381 cm^{-1} respectively, so that the ring tilt ν_{21} occurs at a lower frequency than the M-ring stretch ν_{11}. Since the assignment of ν_4 to 333 cm^{-1} and ν_{16} to 400 cm^{-1} is not questioned, it would follow that the ν_{21} out-of-phase tilt has a lower frequency than the

in-phase tilt ν_{16}. This is inconceivable, and we are led to conclude that the only possible assignment is of ν_{11} to 381 cm^{-1} and ν_{21} to 450 cm^{-1}. The same order is followed in ferrocene. On the basis of the low frequency data we agree that the strongly temperature dependent ruthenocene mode at 130 cm^{-1} should be assigned to ν_6, and ν_{22} would then be at 170 cm^{-1}, observed in the i.r. only.